Chemical Science

ROYAL SOCIETY OF CHEMISTRY

EDGE ARTICLE

View Article Online
View Journal | View Issue

Cite this: *Chem. Sci.*, 2026, **17**, 1203

All publication charges for this article have been paid for by the Royal Society of Chemistry

Received 10th October 2025
Accepted 17th November 2025

DOI: 10.1039/d5sc07853a

rsc.li/chemical-science

Regio-reversed alkenyl–arylation of ynamides *via* 1,3-olefin shift

Saumya Verma,† Manoj Sethi† and Akhila K. Sahoo *

A cationic Pd-catalysed multicomponent reaction enables the regio-reversed alkenyl–arylation of ynamides through a migratory difunctionalization strategy. A stereoselective 1,3-olefin shift of a keteniminium–alkenyl–Pd intermediate governs the carbopalladation pathway, generating a vinylic Pd species that subsequently couples with aryl boronates. This protocol offers streamlined access to highly substituted branched dienes, trienes, and divinyl ethylene (DVE) derivatives with excellent regio- and stereocontrol. The broad substrate scope, scalability, and mechanistic insights highlight the synthetic potential of this transformation. Additionally, the photophysical properties of these conjugated systems were examined, underscoring their potential as functional materials for optoelectronic applications.

Introduction

Transition metal-catalyzed alkyne difunctionalization has emerged as a powerful strategy for assembling structurally complex molecules from simple and readily available feedstock chemicals.[1–7] These transformations offer excellent control over both regio- and stereoselectivity, enabling the modular incorporation of diverse functional groups onto alkyne scaffolds.[1–5] Despite these advances, the diastereoselective synthesis of internally substituted conjugated polyenes remains challenging due to difficulties in achieving precise stereochemical control (Fig. 1B). Traditionally, conjugated polyene systems are accessed *via* cross-coupling strategies that require pre-functionalized alkenyl partners or strained intermediates (Fig. 1A).[7–16] In contrast, alkyne difunctionalization allows for the regioselective introduction of two distinct substituents across a triple bond, either through direct addition (Fig. 1A)[17,18] or *via* migratory mechanisms (Fig. 1A), where one group undergoes positional rearrangement before interception by a second coupling partner.[19–27] These strategies enable the stereoselective assembly of conjugated polyene frameworks, often surpassing traditional cross-coupling approaches in terms of step-economy, selectivity, and overall synthetic efficiency.

In this context, most established difunctionalization strategies for polarized alkynes (ynamides) have centred on hydro-olefination or stepwise olefin incorporation. Seminal contributions from the Skrydstrup[28] and Zhu[29] groups have provided access to polarized diene frameworks (Fig. 1C). However, reports of carbo-olefination in such systems are rare. An

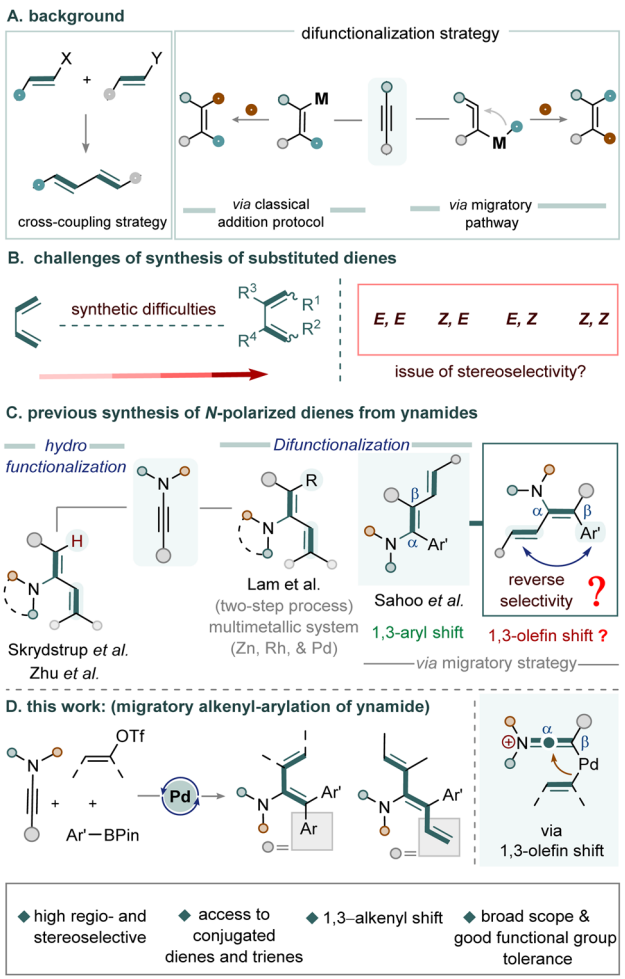

Fig. 1 Background and this work.

School of Chemistry, University of Hyderabad, 500046, India. E-mail: akhilchemistry12@gmail.com; akssc@uohyd.ac.in

† These authors contributed equally.

Table 1 Optimization of reaction conditions[a]

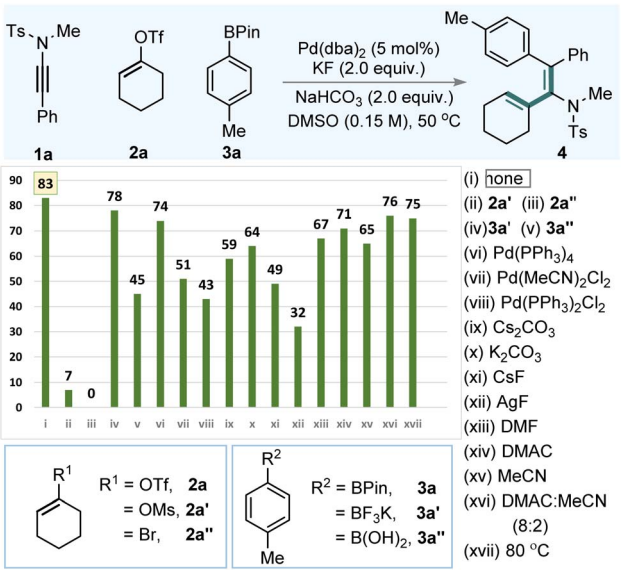

[a] Reaction conditions: **1** (0.05 mmol), **2** (0.075 mmol), **3** (0.075 mmol), $Pd(dba)_2$ (0.005 mmol), KF (0.1 mmol), $NaHCO_3$ (0.1 mmol): DMSO (0.15 M), stirred at 50 °C.

exception is the study by Lam *et al.*, in which a bimetallic Rh/Zn system for oxazolidinone-derived ynamides forms α-vinylic zinc intermediates that couple with iodoalkenyl reagents, furnishing the corresponding carbo-olefination products (Fig. 1C).[30]

We recently reported a one-pot aryl-olefination of ynamides, wherein 1,3-aryl shift governed the reaction pathway, enabling the selective synthesis of substituted linear dienes (Fig. 1C).[19] Building on these findings, we envisaged that reversing the regioselectivity *via* alkenyl–arylation could provide access to branched conjugated olefins, which are challenging to synthesize using existing methods (Fig. 1D). To realize this goal, a successful 1,3-olefin shift is essential. In contrast to the facile 1,3-aryl migrations, olefin rearrangements present significant challenges, primarily due to competing migration pathways and the tendency of *in situ* generated vinylic metal intermediates from alkenyl-electrophile to undergo β-hydride elimination (Fig. 1D).[31–34]

The present study introduces a general one-pot strategy for the synthesis of internally substituted branched diene and triene frameworks through the three-component coupling of ynamides, alkenyl triflates, and aryl boronates with high selectivity. The reaction proceeds under mild, ligand-free conditions, effectively addressing the challenges associated with olefin migration (Fig. 1D).

Results and discussion

To evaluate our hypothesis, ynamide **1a**, cyclohex-1-en-1-yl trifluoromethanesulfonate (**2a**), and 4,4,5,5-tetramethyl-2-(*p*-tolyl)-1,3,2-dioxaborolane (**3a**) were selected as model substrates (Table 1). Reaction optimization revealed that using $Pd(dba)_2$ (5.0 mol%) in combination with KF (2.0 equiv.) and $NaHCO_3$ (2.0 equiv.) in DMSO (0.15 M) at 50 °C delivered the desired alkenyl–arylated product **4** in 83% yield with complete regio- and *syn*-selectivity (Table 1, entry i). Substituting the alkenyl triflate with cyclohex-1-en-1-yl methanesulfonate (**2a′**) or 1-bromocyclohex-1-ene (**2a″**) resulted in significantly reduced yields or complete suppression of product formation (entries ii and iii). Similarly, replacing arylboronate **3a** with boronic acid derivatives **3a′** or **3a″** led to only moderate yields (78% and 45%, entries iv and v). Alternative palladium sources, including various Pd(0) and Pd(II) complexes, did not improve the outcome when compared with $Pd(dba)_2$ (entries vi–viii). Base/additive combinations, such as Cs_2CO_3, K_2CO_3, CsF, and AgF, led to **4** in 32–64% (entries ix–xii). Finally, alterations of solvent system (entries xiii–xvi) or reaction temperature (entry xvii) did not enhance the product yield.

Importantly, the choice of alkenyl electrophile and the solvent system is critical in determining the overall regioselectivity. Labile electrophiles can generate vinylic cationic Pd(II) species that exhibit enhanced electrophilicity stabilized by a coordinating solvent. This promotes the formation of the keteniminium intermediates and the subsequent olefin migration, leading to a regioselective product. Nonetheless, the nature of the ynamide is equally crucial; directing-enabled ynamides (**1h**) can result in the formation of regioisomeric mixtures.

Under the optimized conditions, the scope of this three-component protocol for synthesizing branched 1,3-dienes was explored (Scheme 1a). The *para*-substituted arylboronates bearing electron-donating groups *p*-Me (**3a**) and *p*-OMe (**3b**) reacted independently with **1a** and **2a** to afford dienes **4** and **5** in 83% and 63% yield, respectively. Despite the potential for Pd deactivation by hydroxyl coordination, the reaction of OH-

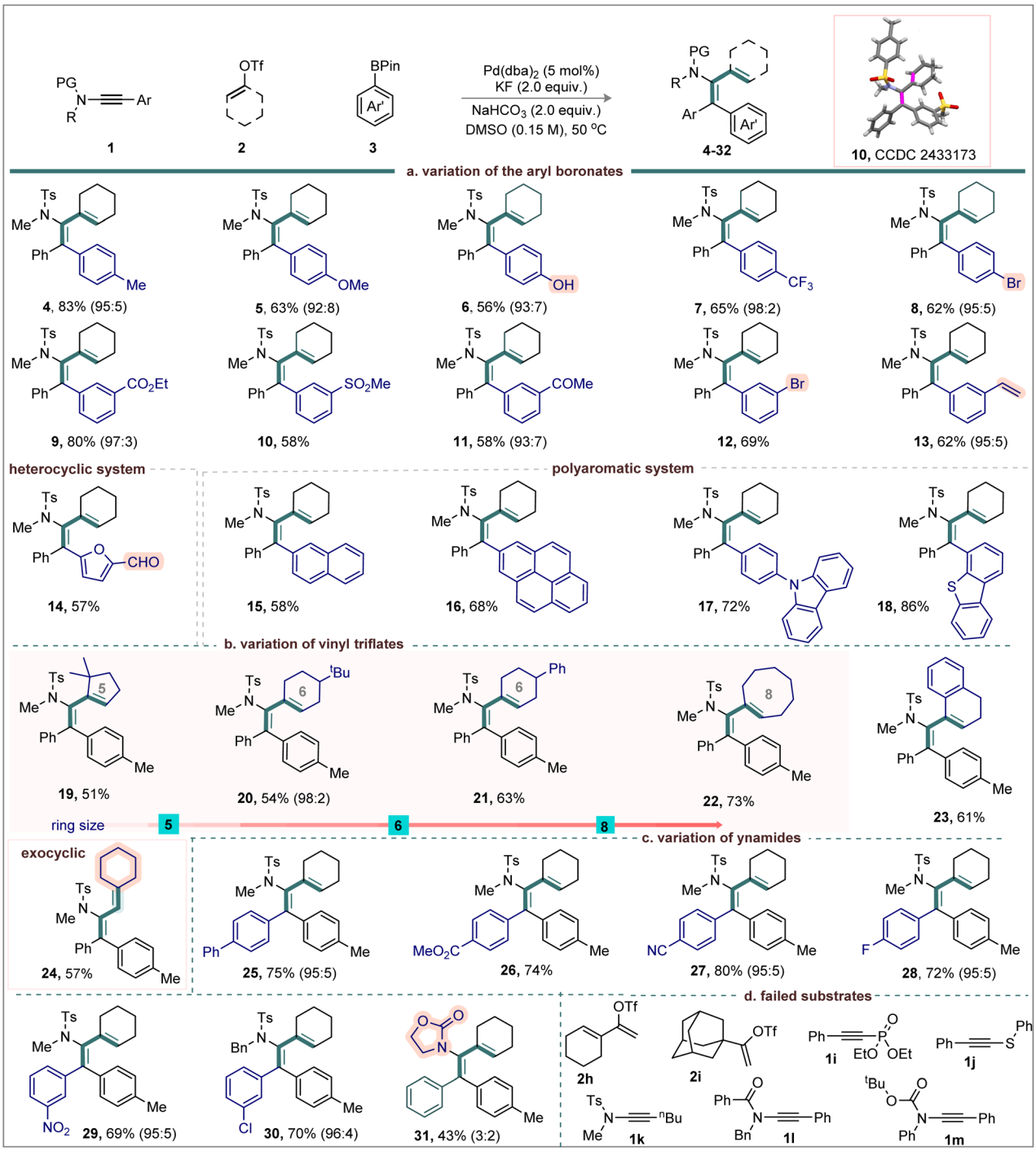

Scheme 1 Scope of reaction; reaction conditions: **1** (0.3 mmol), **2** (0.45 mmol), **3** (0.45 mmol), $Pd(dba)_2$ (0.015 mmol), KF (0.6 mmol), $NaHCO_3$ (0.6 mmol): DMSO (0.15 M), stirred at 50 °C. The regioisomeric ratio (calculated using ^1H NMR) of the products is mentioned in parentheses.

substituted boronate **3c** delivered diene **6** in moderate yield, offering a handle for further derivatization. Electron-deficient and halo-substituted arylboronates, including [*p*-CF_3 (**3d**), *p*-Br (**3e**), and *m*-Br (**3i**)] were well tolerated, furnishing dienes **7** (65%), **8** (62%), and **12** (69%) with the bromo group intact. This highlights the potential for downstream cross-coupling or late-stage functionalization. Likewise, the *meta*-substituted arylboronates [*m*-CO_2Et (**3f**), *m*-SO_2Me (**3g**), *m*-Ac (**3h**), and *m*-Br (**3i**)] also showed broad compatibility delivering **9–12** in 58–80% yield with high regioselectivity. The structure of diene **10** was unambiguously confirmed by single-crystal X-ray diffraction (CCDC 2433173). Notably, the transformation with *m*-vinyl-substituted arylboronate **3j** was smooth affording diene **13** in 62% yield; the vinylic moiety did not affect the reaction outcome. Heteroaryl (**3k**) and polyaromatic substrates (**3l–3o**)

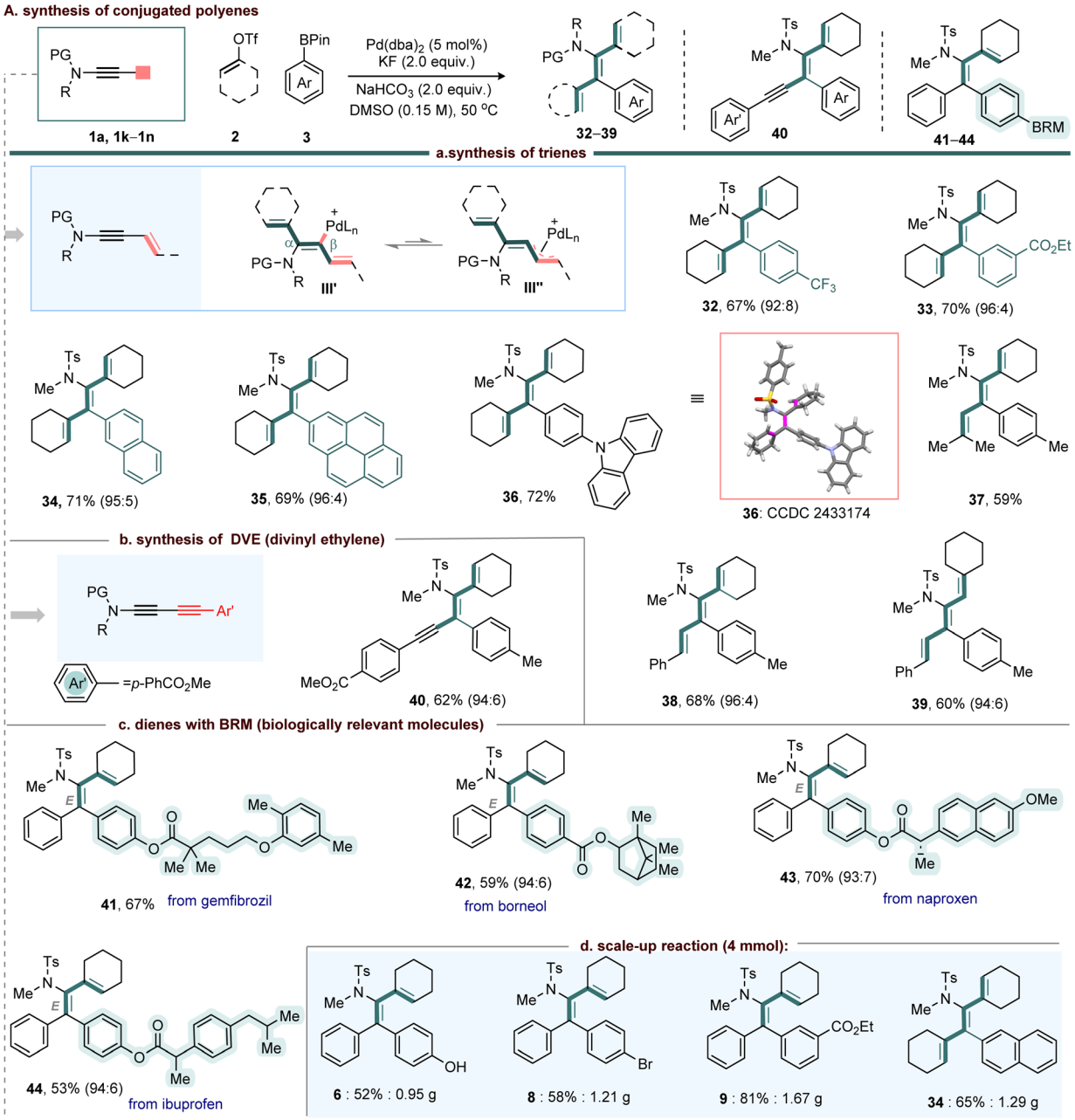

Scheme 2 Scope of reaction and scale-up reaction; reaction conditions: **1** (0.3 mmol), **2** (0.45 mmol), **3** (0.45 mmol), $Pd(dba)_2$ (0.015 mmol), KF (0.6 mmol), $NaHCO_3$ (0.6 mmol): DMSO (0.15 M), stirred at 50 °C. The regioisomeric ratio (calculated using ^1H NMR) of the products is mentioned in parentheses.

participated efficiently in the reaction delivering the desired products **14–18** in 57–86% yield.

We next examined the reactivity of alkenyl triflates (Scheme 1b). Gratifyingly, both cyclic and acyclic variants of alkenyl triflates coupled efficiently with **1a** and **3a**, delivering the corresponding 1,3-dienes with excellent stereoselectivity. The sterically demanding cyclic systems, including five-to eight-membered alkenyl triflates (**2b–2e**) were participated smoothly in the *syn*-olefinic–arylation of ynamides; the respective products **19–22** were obtained in moderate to good yields (51–73%). Likewise, products **23** (61%), and **24** (57%) were made from the coupling of alkenyl triflates derived from tetralone (**2f**), and exocyclic framework (**2g**), respectively.

We then turned our attention to study the ynamides scope (Scheme 1c). Aryl-substituted ynamides bearing both electron-donating and electron-withdrawing groups, such as *p*-Ph (**1b**), *p*-CO_2Me (**1c**), *p*-CN (**1d**), *p*-F (**1e**), *m*-NO_2 (**1f**), and *m*-Cl (**1g**) reacted efficiently to furnish the corresponding products **25–30** in good yields (69–80%). In contrast, the oxazolidinone ynamide **1h** proved less effective, delivering product **31** in 43% yield with poor regioselectivity (3 : 2). This reduced efficiency is likely due to the combined influence of the oxazolidinone directing group

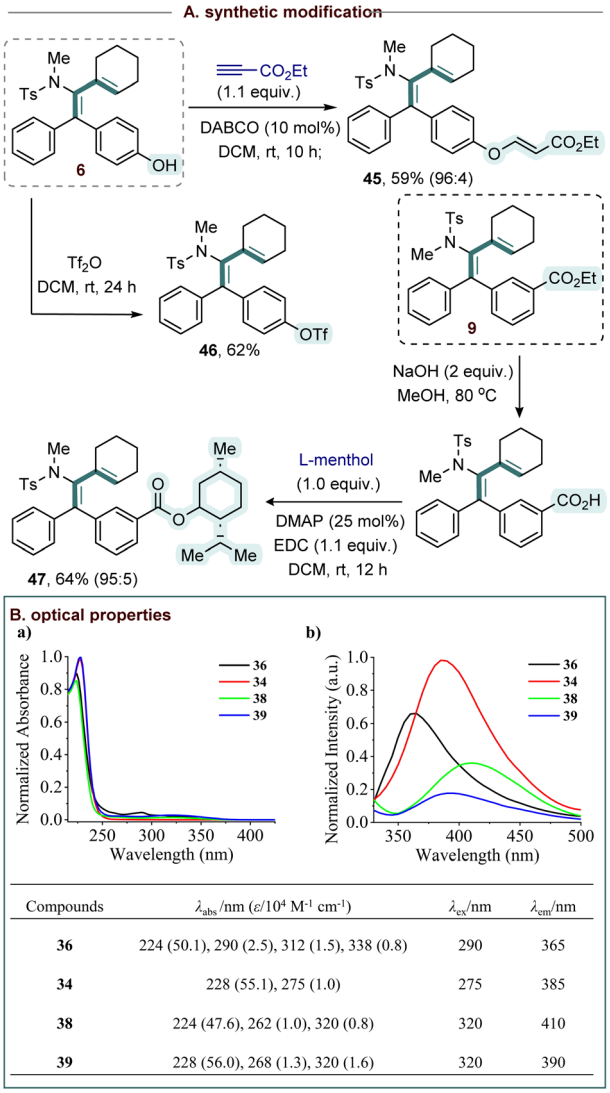

Compounds	λ_{abs}/nm (ε/10^4 M^{-1} cm^{-1})	λ_{ex}/nm	λ_{em}/nm
36	224 (50.1), 290 (2.5), 312 (1.5), 338 (0.8)	290	365
34	228 (55.1), 275 (1.0)	275	385
38	224 (47.6), 262 (1.0), 320 (0.8)	320	410
39	228 (56.0), 268 (1.3), 320 (1.6)	320	390

Scheme 3 Synthetic application and photophysical study; (a) absorption (5 μM, λ_{abs}) and (b) emission (50 μM, λ_{em}) spectra of the compounds were investigated in MeCN at 298K. The emission spectra were measured upon excitation at 275–320 nm.

and the intrinsic electronic character of the ynamide. Unfortunately, the triflate electrophiles 1-(cyclohex-1-en-1-yl)vinyl triflate (**2h**) and adamantanyl vinyl triflate (**2i**) did not undergo the desired transformation with **1a** and **3a**, resulting in a complex mixture. The outcome with **2h** can be attributed to multiple competing migration pathways, whereas for bulky **2i**, steric hindrance between the ynamide *N*-tosyl group and the electrophile likely prevents the intramolecular 1,3-olefin shift. In addition, other alkyne derivatives such as diethyl (phenylethynyl)phosphonate (**1i**), and phenyl(phenylethynyl)sulfane (**1j**) failed to deliver the desired diene products under the standard conditions (Scheme 1d).

To further demonstrate the versatility of this synthetic method, we extended its application to the synthesis of conjugated trienes using ene-ynamides (Scheme 2). The dual functionality of ene-ynamides, comprising both alkyne and alkene moieties, poses site-selectivity challenges. Specifically, the formation of a π–allyl–Pd intermediate (**III″**) from the reaction intermediate **III′** could complicate the reaction pathway (Scheme 2a). However, the nucleophilic β-carbon of the ynamide strengthens the Pd–C bond, which suppresses π–allyl–Pd formation and consequently directs the reaction toward the selective synthesis of conjugated trienes (Scheme 2a).

In this context, a variety of aryl boronates including *para*-(**3d**) and *meta*-substituted (**3f**) derivatives, as well as polyaromatics (**3l–3n**) were subjected to standard conditions with cyclic ene-ynamide **1k** and alkenyl triflate **2a**, delivering trienes **32–36** in 67–72% yield. Further, acyclic ene-ynamide (**1l** and **1m**) reacted smoothly furnishing trienes **37–39** in 59–68% yield.

We next examined the reactivity of yne-ynamides (**1n**) under the standard conditions. Remarkably, despite the coexistence of two potentially reactive sites the ynamide and the terminal alkyne, the transformation proceeded with complete chemoselectivity at the ynamide moiety, affording the highly substituted DVE derivative **40** in 62% yield.

Furthermore, the reaction exhibited excellent tolerance toward a wide range of structurally complex scaffolds incorporated at the periphery of the aryl-boronate unit. Derivatives of gemfibrozil (**3p**), borneol (**3q**), naproxen (**3r**), and ibuprofen (**3s**) reacted smoothly with **1a** and **2a**, delivering products **41–44** in 53–70% yield with good selectivity (Scheme 2c).

To our delight, the reaction was successfully performed on a gram scale (Scheme 2d). Specifically, the reaction of the corresponding ynamides (4.0 mmol) with alkenyl triflates and aryl boronates under the standard conditions afforded compounds **6** (0.95 g, 52%), **8** (1.21 g, 58%), **9** (1.67 g, 81%), and **34** (1.29 g, 65%). Notably, these yields are consistent with those obtained in the small-scale experiments, demonstrating the scalability and robustness of the protocol.

To demonstrate the synthetic versatility of the method, further functionalization of selected compounds was carried out (Scheme 3A). Treating compound **6** with ethyl propiolate led to the product **45** in 59% yield. The hydroxyl group in **6** was readily protected providing the complex aryl triflate **46** in 62% yield, thereby offering a handle for further derivatization. The ester hydrolysis of compound **9** provided carboxylic acid, which was then coupled with L-menthol to deliver ester **47** in 64% yield (Scheme 3A).

Next, the photophysical properties such as absorption and emission spectra of the compounds (**36**, **34**, **38** and **39**) were studied in acetonitrile (MeCN) at 298 K (Scheme 3B). The compounds displayed intense high-energy bands at 224–228 nm, assigned to allowed π → π* intra-ligand transitions within the aromatic framework. Less intensity features in the 262–338 nm region are assignable to n → π* transitions from nitrogen lone pairs to π* orbitals, and lower-energy π → π* excitations involving extended aromatic conjugation. The emission spectra of compounds (**36**, **34**, **38** and **39**) were recorded in MeCN upon excitation at 290, 275, and 320 nm. All compounds exhibited emission in the near-UV to blue region (365–410 nm) having emission maxima at 365, 385, 410, and 390 nm, respectively. These photophysical features highlight the potential of the synthesized conjugated frameworks as

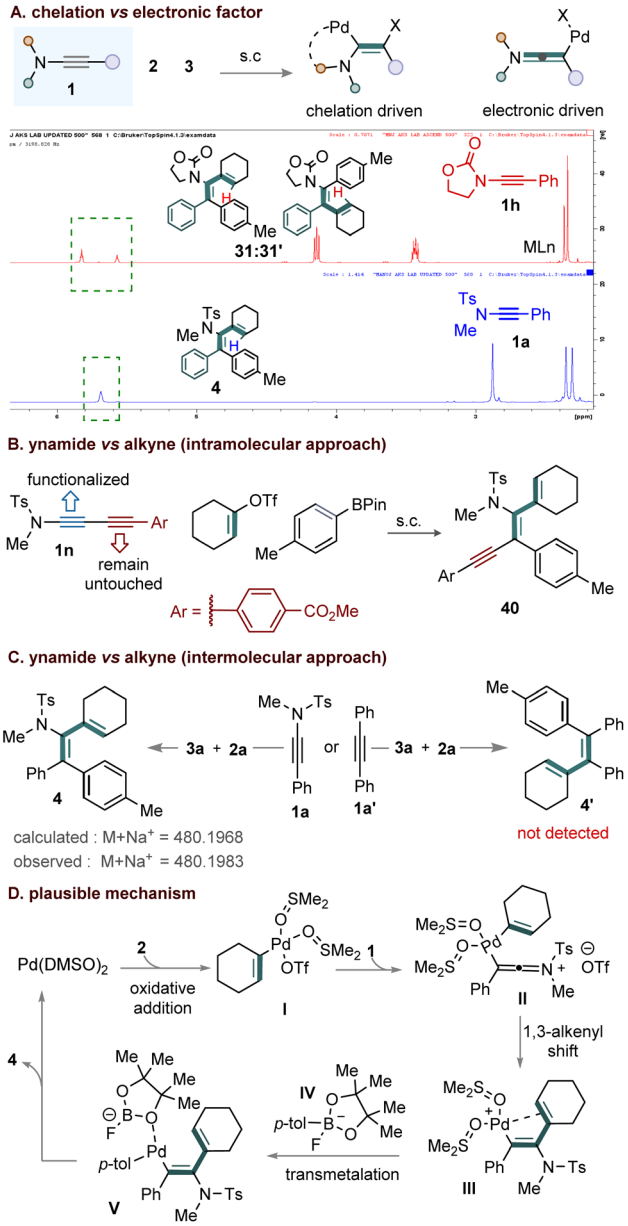

Scheme 4 Control experiment and plausible mechanism.

functional materials for optoelectronic applications, and UV-absorbing materials.[7]

To probe the reaction mechanism and factors controlling regioselectivity, a series of control experiments were conducted, including a competitive reaction between ynamides **1a** and **1h** with **2a** and **3a** under standard conditions (Scheme 4A). The reaction afforded products **4** (83%) and **31** (43%) in a 3 : 2 regioisomeric ratio. The exclusive formation of diene **4** from **1a** suggests that *N*-lone pair delocalization directs regioselectivity, whereas the formation of regioisomer **31** from *N*-oxazolidinone-substituted ynamide **1h** highlights the competing influence of chelation and electronic effects on the reaction outcome.

Crossover experiments were performed under the optimized conditions to probe chemoselectivity (Scheme 4B and 4C). In the intramolecular case, yne-ynamide **1l** reacted exclusively to give product **40**, confirming preferential reactivity of the ynamide moiety even when conjugated with an alkyne (Scheme 4B). While in the intermolecular crossover experiment, the reaction independently performed among **1a**/**1a′** with **2a** and **3a**, the product **4** was only formed from ynamide **1a** (Scheme 4C). These results clearly highlight the preferential reactivity of the ynamide moiety over the alkyne unit (Scheme 4B and 4C).

Based on experimental results and literature precedents, a plausible mechanism is proposed (Scheme 4D). Ligand exchange between $Pd(dba)_2$ and DMSO generates $Pd(0)(DMSO)_2$, which undergoes oxidative addition with alkenyl triflate **2** to form a cationic alkenyl-Pd(II) intermediate **I**. Nucleophilic attack of ynamide **1** on **I**, with concomitant triflate displacement, furnishes keteniminium intermediate **II**. A stereoselective intramolecular 1,3-olefin shift then produces intermediate **III**. Transmetalation of **III** with the aryl fluoroborate **IV** in the presence of KF forms alkenyl-Pd-aryl species **V**, which undergoes reductive elimination to deliver the final product **4**.

Conclusions

In conclusion, we have developed a Pd-catalyzed regio-reversed dicarbofunctionalization strategy of ynamides, enabling highly selective 1,2-alkenylarylation *via* a stereoselective 1,3-olefin shift. This transformation proceeds through a cationic alkenyl-Pd intermediate, which is efficiently intercepted by aryl boronic esters to furnish α-alkenylated, branched conjugated dienes and trienes with excellent regio- and stereocontrol. The method exhibits broad substrate scope and high tolerance toward various functional groups. This transformation also offers an efficient route for the synthesis of complex π-conjugated systems, including divinyl ethylene (DVE) derivatives. Furthermore, the detailed photophysical studies of the compounds revealed strong π → π* and n → π* absorption and features fluorescence emission in the near-UV to blue region (365–410 nm). These findings suggest that the conjugated frameworks possess strong potential for use as functional materials in optoelectronic devices and UV-absorbing systems. This work not only expands the synthetic utility of ynamides in transition-metal catalysis but also introduces new avenues for the synthesis of divinyl ethylene (DVE) derivatives and their application to showcasing the distinctive photophysical behaviour.

Author contributions

All authors have approved the final version of the manuscript. A. K. S., M. S., and S. V. conceived the idea and M. S. and S. V. performed the experiments. Review, editing and supervision done by A. K. S.

Conflicts of interest

There are no conflicts to declare.

Data availability

CCDC 2433173 (**10**) and CCDC 2433174 (**36**) contain the supplementary crystallographic data for this paper.[35a,b]

The data supporting this article have been included as part of the supplementary information (SI). Supplementary information is available. See DOI: **https://doi.org/10.1039/d5sc07853a**.

Acknowledgements

We thank University of Hyderabad (UoH; UPE-CAS and PURSE-FIST) for the overall facility. M. S. thank UGC for fellowship. We thank Mr Mahesh Srichand Rathod for the help in solving the X-ray crystal data. We also thank Aryan Gautam from Jawaharlal Nehru University, New Delhi for photophysical studies.

Notes and references

1 J. Corpas, P. Mauleón, R. G. Arrayás and J. C. Carretero, *ACS Catal.*, 2021, **11**, 7513–7551.
2 F. Alonso, I. P. Beletskaya and M. Yus, *Chem. Rev.*, 2004, **104**, 3079–3108.
3 U. Wille, *Chem. Rev.*, 2013, **113**, 813–853.
4 X.-M. Nong, A. Gu, S. Zhai, J. Li, Z.-Y. Yue, M.-Y. Li and Y. Liu, *iScience*, 2024, **27**, 109223.
5 R. Chinchilla and C. Najera, *Chem. Rev.*, 2014, **114**, 1783–1826.
6 M. Sethi, S. Dutta and A. K. Sahoo, *Org. Lett.*, 2024, **26**, 3224–3229.
7 S. Dutta, M. Sethi, A. Maity, A. Sahoo, V. Gandon and A. K. Sahoo, *Org. Chem. Front.*, 2024, **11**, 7168–7175.
8 J. Ahmed, G. C. Haug, V. D. Nguyen, A. Porey, R. Trevino and O. V. Larionov, *Synthesis*, 2023, **55**, 1642–1651.
9 J. Corpas, P. Mauleón, R. G. Arrayás and J. C. Carretero, *J. Am. Chem. Soc.*, 2013, **135**, 6747–6750.
10 M. De Paolis, I. Chataigner and J. Maddaluno, *Top. Curr. Chem.*, 2012, **327**, 87.
11 J. Corpas, P. Mauleón, R. G. Arrayás and J. C. Carretero, *J. Am. Chem. Soc.*, 2015, **137**, 6747–6750.
12 E. M. Woerly, J. Roy and M. D. Burke, *Nat. Chem.*, 2014, **6**, 484–491.
13 X.-H. Hu, J. Zhang, X.-F. Yang, Y. H. Xu and T.-P. Loh, *J. Am. Chem. Soc.*, 2015, **137**, 3169–3172.
14 S. J. Lee, T. M. Anderson and M. D. Burke, *Angew. Chem., Int. Ed.*, 2010, **49**, 8860–8863.
15 J. Li, S. G. Ballmer, E. P. Gillis, S. Fujii, M. J. Schmidt, A. M. E. Palazzolo, J. W. Lehmann, G. F. Morehouse and M. D. Burke, *Science*, 2015, **347**, 1221–1226.
16 J. Li, A. S. Grillo and M. D. Burke, *Acc. Chem. Res.*, 2015, **48**, 2297–2307.
17 S. Chen, Y.-N. Wang, J. Xie, W. Li, M. Ye, X. Ma, K. Yang, S. Li, Y. Lan and Q. Song, *Nat. Commun.*, 2024, **15**, 5479.
18 T. Long, C. Zhu, L. Li, L. Shao, S. Zhu, M. Rueping and L. Chu, *Nat. Commun.*, 2023, **14**, 55.
19 R. Vanjari, S. Dutta, S. Yang, V. Gandon and A. K. Sahoo, *Org. Lett.*, 2022, **24**, 1524–1529.
20 M. P. Gogoi, R. Vanjari, B. Prabagar, S. Yang, S. Dutta, R. K. Mallick, V. Gandon and A. K. Sahoo, *Chem. Commun.*, 2021, **57**, 7521–7524.
21 S. Dutta, R. K. Mallick and A. K. Sahoo, *Angew. Chem., Int. Ed.*, 2023, **62**, e202300816.
22 F. Zhao, D. Zhang, Y. Nian, L. Zhang, W. Yang and H. Liu, *Org. Lett.*, 2014, **16**, 5124–5127.
23 G. Zhang, B. Feng, Y. Wang, J. Chen, X. Ma and Q. Song, *Org. Lett.*, 2024, **26**, 3109–3113.
24 K. Jana, A. Bhunia and A. Studer, *Chem*, 2020, **6**, 512–522.
25 P. Dominguez-Molano, A. Solé-Daura, J. J. Carbó and E. Fernández, *Adv. Sci.*, 2024, **11**, 2309779.
26 P. Domínguez-Molano, R. Weeks, R. J. Maza, J. J. Carbó and E. Fernández, *Angew. Chem., Int. Ed.*, 2023, **62**, e202304791.
27 X. Tang and A. Studer, *Angew. Chem., Int. Ed.*, 2018, **57**, 814–817.
28 A. T. Lindhardt, M. L. H. Mantel and T. Skrydstrup, *Angew. Chem., Int. Ed.*, 2008, **47**, 2668–2672.
29 Y. Yang, L. Wang, J. Zhang, Y. Jin and G. Zhu, *Chem. Commun.*, 2014, **50**, 2347–2349.
30 B. Gourdet, M. E. Rudkin, C. A. Watts and H. W. Lam, *J. Org. Chem.*, 2009, **74**, 7849–7858.
31 H. Huang, L. Tang, Y. Xi, G. He and H. Zhu, *Tetrahedron Lett.*, 2016, **57**, 1873–1876.
32 P. Bao, H. Xiao, Q. Li, Y. Wang, Y. Wang and G. He, *Org. Biomol. Chem.*, 2025, **23**, 5821–5825.
33 D. Zhang, J. Man, Y. Chen, L. Yin, J. Zhong and Q.-F. Zhang, *RSC Adv.*, 2019, **9**, 12567–12571.
34 G. Evano, B. Michelet and C. Zhang, *C. R. Chim.*, 2017, **20**, 648–664.
35 (*a*) CCDC 2433173: Experimental Crystal Structure Determination, 2025, DOI: **10.5517/ccdc.csd.cc2mnxgp**; (*b*) CCDC 2433174: Experimental Crystal Structure Determination, 2025, DOI: **10.5517/ccdc.csd.cc2mnxhq**.